Numerical Algorithms
https://doi.org/10.1007/s11075-022-01269-z
ORIGINAL PAPER

A formal construction of a divergence-free basis in the nonconforming virtual element method for the Stokes problem

Do Y. Kwak[1] · **Hyeokjoo Park**[1]

Received: 12 August 2021 / Accepted: 27 January 2022

Abstract

We develop a formal construction of a pointwise divergence-free basis in the nonconforming virtual element method of arbitrary order for the Stokes problem introduced in Zhao et al. (*SIAM J. Numer. Anal.* 57(6):2730–2759, 2019). The proposed construction can be seen as a generalization of the divergence-free basis in Crouzeix-Raviart finite element space (Brenner, *Math. Comp.* 55(192):411–437, 1990; Thomasset, 1981) to the virtual element space. Using the divergence-free basis obtained from our construction, we can eliminate the pressure variable from the mixed system and obtain a symmetric positive definite system. Several numerical tests are presented to confirm the efficiency and the accuracy of our construction.

Keywords Nonconforming virtual element method · Stokes problem · Polygonal mesh · Divergence-free element

Mathematics Subject Classification (2010) 65N12 · 65N30 · 76D07

1 Introduction

Recently, the virtual element method (VEM) was proposed in [5] as a generalization of the finite element method (FEM) to general polygonal and polyhedral meshes. In VEMs, the local discrete spaces on the mesh polygons/polyhedrons, called local virtual element spaces, consist of polynomials of certain degrees and some other

✉ Do Y. Kwak
kdy@kaist.ac.kr

Hyeokjoo Park
hjpark235@kaist.ac.kr

1 Department of Mathematical Sciences, Korea Advanced Institute of Science and Technology, Daejeon, 34141, Korea

Published online: 17 February 2022

non-polynomial functions that are solutions of specific partial differential equations. Although such functions are not defined explicitly, they are characterized by degrees of freedom, such as values at mesh vertices, the moments on mesh edges/faces, and the moments on mesh polygons/polyhedrons. On each (polygonal or polyhedral) element, the discrete bilinear form can be computed using only the degrees of freedom, and satisfies two properties, called consistency and stability. Here the consistency means that the discrete bilinear form is equal to the continuous bilinear form when one of the arguments is a polynomial, and the stability means that the discrete bilinear form is coercive for general virtual elements. Moreover, the virtual element spaces can be extended to arbitrary order in straightforward way. Because of such advantages, VEMs have been developed for many different types of equations, and successfully applied to various problems. The authors in [4] presented nonconforming VEMs for elliptic problems. In [17], the conforming and nonconforming VEMs for general elliptic problems were proposed. Various VEMs for solving linear elasticity problems can be found in [9, 22, 25, 27]. In [6–8, 13], VEMs for magnetostatic problems and Maxwell's equations were presented. The authors in [15] constructed $\boldsymbol{H}(\mathrm{div})$-conforming virtual elements and presented mixed VEMs for Darcy flow. Conforming and nonconforming VEMs for elliptic eigenvalue problems were studied in [20, 21], respectively. For more thorough survey, we refer to [1, 3–5, 10, 11, 15, 19, 28] and references therein.

There have appeared some results concerning the VEMs for the Stokes problem as well. In [2], a stream formulation of the VEM for the Stokes problem was presented. In [16, 23], the nonconforming VEM of arbitrary order for the Stokes problem on polygonal and polyhedral meshes was first introduced. Therein, each component of the velocity is approximated by the nonconforming virtual element space presented in [4]. However, the velocity approximation in [16, 23] is not pointwise divergence-free, and it is merely divergence-free in a relaxed (projected) sense.

In the two-dimensional case, some researchers have developed VEMs for the Stokes problem in which the velocity approximation is pointwise divergence-free. In [12], the divergence-free velocity approximation is presented in the conforming virtual element space of order $k \geq 2$. On each polygon, the virtual element space consists of velocity solutions of the local Stokes problem with Dirichlet boundary condition. On the other hand, the nonconforming virtual element space of arbitrary order was constructed by enriching a $\boldsymbol{H}(\mathrm{div})$-conforming virtual element space in [29]. However, the proposed methods in [12, 29] only showed that the computed velocity approximation is pointwise divergence-free. They do not discuss the construction of divergence-free basis functions. To the best of our knowledge, a formal construction of divergence-free bases in these VEMs has never been considered and developed.

The main goal of this paper is to present a formal construction of a divergence-free basis in the two-dimensional nonconforming VEMs for the Stokes problem introduced in [29]. We first compute the dimension of the divergence-free subspace of the nonconforming virtual element space, using Euler's formula. We then construct basis functions of the subspace, in a similar fashion to the divergence-free basis functions proposed in [14, 26] but we generalize to polygonal meshes and higher-order virtual elements. Using the construction of a divergence-free basis, we can eliminate the pressure variable from the coupled system and reduce the saddle point problem to a symmetric positive definite system having fewer unknowns in velocity variable only. Although we only consider the Stokes problem in this paper, we expect that our construction can be applied to more complicated problems, such as the incompressible Navier-Stokes problem.

The rest of this paper is organized as follows. In Section 2, we state the stationary Stokes problem and its variational formulation. In Section 3, we review the divergence-free nonconforming VEM for the Stokes problem introduced in [29]. In Section 4, we discuss a formal construction of divergence-free basis of the nonconforming virtual element space. In Section 5, we discuss implementations including nonhomogeneous Dirichlet boundary conditions. In Section 6, we offer some numerical experiments that verify the efficiency and the accuracy of our construction. Finally, conclusions are given in Section 7.

2 Model problem

Let $\Omega \subset \mathbb{R}^2$ be a bounded, convex polygonal domain with boundary $\partial\Omega$. We consider the Stokes problem on Ω: Given $\boldsymbol{f} : \Omega \to \mathbb{R}^2$ and $\boldsymbol{g} : \partial\Omega \to \mathbb{R}^2$, find $\boldsymbol{u} : \Omega \to \mathbb{R}^2$ and $p : \Omega \to \mathbb{R}$ such that

$$\begin{cases} -\Delta \boldsymbol{u} + \nabla p = \boldsymbol{f} & \text{in} \quad \Omega, \\ \operatorname{div} \boldsymbol{u} = 0 & \text{in} \quad \Omega, \\ \boldsymbol{u} = \boldsymbol{g} & \text{on} \quad \partial\Omega. \end{cases} \tag{1}$$

In order to obtain the variational formulation of (1), we introduce the usual notation for Sobolev spaces, norms, seminorms, and inner products. Let D be a bounded domain in $\mathbb{R}^2$. We then define $\boldsymbol{L}^2(D) = [L^2(D)]^2$ and $\boldsymbol{H}^s(D) = [H^s(D)]^2$ for $s > 0$. The L^2-inner product of $L^2(D)$ and $\boldsymbol{L}^2(D)$ is denoted by $(\cdot,\cdot)_{0,D}$. Next, for $s \geq 0$, the H^s-norm of $H^s(D)$ and $\boldsymbol{H}^s(D)$ is denoted by $\|\cdot\|_{s,D}$. Similarly, for $s > 0$, the H^s-seminorm of $H^s(D)$ and $\boldsymbol{H}^s(D)$ is denoted by $|\cdot|_{s,D}$. The subspace $L_0^2(D)$ of $L^2(D)$ is defined by

$$L_0^2(D) = \left\{ q \in L^2(D) : \int_D q \mathrm{d}\boldsymbol{x} = 0 \right\}.$$

Let us define

$$\begin{aligned} \boldsymbol{H}_0^1(\Omega) &= \{\boldsymbol{v} \in \boldsymbol{H}^1(\Omega) : \boldsymbol{v} = \boldsymbol{0} \text{ on } \partial\Omega\}, \\ \boldsymbol{H}_{\boldsymbol{g}}^1(\Omega) &= \{\boldsymbol{v} \in \boldsymbol{H}^1(\Omega) : \boldsymbol{v} = \boldsymbol{g} \text{ on } \partial\Omega\}. \end{aligned}$$

Then, the variational form of the Stokes problem (1) is written as follows: For a given $\boldsymbol{f} \in \boldsymbol{L}^2(\Omega)$ and a given $\boldsymbol{g} \in \boldsymbol{H}^{1/2}(\partial\Omega)$ satisfying

$$\int_{\partial\Omega} \boldsymbol{g} \cdot \boldsymbol{n}_\Omega \mathrm{d}s = 0 \tag{2}$$

where $\boldsymbol{n}_\Omega$ is the unit normal vector on $\partial\Omega$ in the outward direction with respect to Ω, find $\boldsymbol{u} \in \boldsymbol{H}^1_{\boldsymbol{g}}(\Omega)$ and $p \in L^2_0(\Omega)$ such that

$$\begin{cases} a(\boldsymbol{u}, \boldsymbol{v}) + b(\boldsymbol{v}, p) = & (\boldsymbol{f}, \boldsymbol{v})_{0,\Omega} \quad \forall \boldsymbol{v} \in \boldsymbol{H}^1_0(\Omega), \\ \qquad\qquad b(\boldsymbol{u}, q) = & 0 \qquad\qquad\quad \forall q \in L^2_0(\Omega), \end{cases} \tag{3}$$

where

$$a(\boldsymbol{u}, \boldsymbol{v}) = \int_\Omega \nabla \boldsymbol{v} : \nabla \boldsymbol{u} \mathrm{d}\boldsymbol{x}, \quad b(\boldsymbol{v}, q) = -\int_\Omega q \operatorname{div} \boldsymbol{v} \, \mathrm{d}\boldsymbol{x}. \tag{4}$$

The functions $\boldsymbol{u}$ and p are called velocity and pressure, respectively.

3 Divergence-free nonconforming VEM for the stokes problem

In this section, we summarize some preliminaries and review the divergence-free nonconforming VEM for the Stokes problem introduced in [29].

3.1 Notations and preliminaries

Let $\{\mathcal{P}_h\}_h$ be a family of decompositions (meshes) of the domain Ω into polygonal elements K with maximum diameter h. We assume that the decompositions satisfy the following regularity properties [4, 5, 12, 29].

Assumption 1 There exists $\rho > 0$ independent of h such that

- the decomposition $\mathcal{P}_h$ consists of a finite number of nonoverlapping convex polygonal elements;
- if $K \in \mathcal{P}_h$ and e is an edge of K then $h_e \geq \rho h_K$, where h_e and h_K denote the diameter of e and K, respectively;
- every element K of $\mathcal{P}_h$ is star-shaped with respect to the ball of radius ρh_K.

We next define some notations for sets of mesh items. We denote by $\mathcal{V}_h$ and $\mathcal{E}_h$ the set of all mesh vertices and mesh edges in $\mathcal{P}_h$, respectively. We also denote by $\mathcal{V}^i_h$ and $\mathcal{V}^\partial_h$ the set of all mesh vertices in the internal and the boundary of $\mathcal{P}_h$, respectively. Similarly $\mathcal{E}^i_h$ is the set of all mesh edges in the internal of $\mathcal{P}_h$, and $\mathcal{E}^\partial_h$ the set of all mesh edges in the boundary of $\mathcal{P}_h$. We also define

$$\begin{aligned} N_P &= \text{the number of polygons in } \mathcal{P}_h, \\ N_E &= \text{the number of edges in } \mathcal{E}_h, \\ N_{E,i} &= \text{the number of edges in } \mathcal{E}^i_h, \\ N_{E,\partial} &= \text{the number of edges in } \mathcal{E}^\partial_h, \\ N_V &= \text{the number of vertices in } \mathcal{V}_h, \\ N_{V,i} &= \text{the number of vertices in } \mathcal{V}^i_h, \\ N_{V,\partial} &= \text{the number of vertices in } \mathcal{V}^\partial_h. \end{aligned}$$

For each $K \in \mathcal{P}_h$, let $\boldsymbol{n}_K$ and $\boldsymbol{t}_K$ denote its exterior unit normal vector and counterclockwise tangential vector, respectively. Let $e \in \mathcal{E}_h^i$. We then define respectively $\boldsymbol{n}_e$ and $\boldsymbol{t}_e$ as the unit normal and tangential vector of e with orientation fixed once and for all. Next let $e \in \mathcal{E}_h^\partial$, we define respectively $\boldsymbol{n}_e$ and $\boldsymbol{t}_e$ as the unit normal and tangential vector on e in the outward and counterclockwise direction with respect to Ω.

Let $e \in \mathcal{E}_h^i$ and let K^- and K^+ be the polygons in $\mathcal{P}_h$ that have e as a common edge, and satisfy $\boldsymbol{n}_e = \boldsymbol{n}_{K_+}$ on e (i.e., $\boldsymbol{n}_e$ points from K^+ to K^-). If $e \in \mathcal{E}_h^\partial$, we define $\boldsymbol{n}_e$ by the unit normal vector in the outward direction with respect to Ω.

Again let $e \in \mathcal{E}_h^i$ and let K^- and K^+ be the polygons in $\mathcal{P}_h$ having e as a common edge. For $\boldsymbol{v} : \Omega \to \mathbb{R}^2$ satisfying $\boldsymbol{v}|_{K^+} \in \boldsymbol{H}^1(K^+)$ and $\boldsymbol{v}|_{K^-} \in \boldsymbol{H}^1(K^-)$, we define the jump of $\boldsymbol{v}$ on the edge e by

$$[\boldsymbol{v}]_e = \boldsymbol{v}|_{K^+}(\boldsymbol{n}_e \cdot \boldsymbol{n}_{K^+}) + \boldsymbol{v}|_{K^-}(\boldsymbol{n}_e \cdot \boldsymbol{n}_{K^-}).$$

If $e \in \mathcal{E}_h^\partial$, we define $[\boldsymbol{v}]_e = \boldsymbol{v}|_e$.

We define the broken Sobolev space $\boldsymbol{H}^1(\Omega; \mathcal{P}_h)$ by

$$\boldsymbol{H}^1(\Omega; \mathcal{P}_h) = \{\boldsymbol{v} \in \boldsymbol{L}^2(\Omega) : \boldsymbol{v}|_K \in \boldsymbol{H}^1(K)\ \forall K \in \mathcal{P}_h\}$$

and define its norm and seminorm by

$$\|\boldsymbol{v}\|_{1,h} = \left(\sum_{K \in \mathcal{P}_h} \|\boldsymbol{v}\|_{1,K}^2\right)^{1/2}, \quad |\boldsymbol{v}|_{1,h} = \left(\sum_{K \in \mathcal{P}_h} |\boldsymbol{v}|_{1,K}^2\right)^{1/2}.$$

We also define

$$\boldsymbol{H}^{1,nc}(\Omega; \mathcal{P}_h) = \left\{\boldsymbol{v} \in \boldsymbol{H}^1(\Omega; \mathcal{P}_h) : \int_e [\boldsymbol{v}]_e \cdot \boldsymbol{q}\, \mathrm{d}\boldsymbol{x} = 0\ \forall \boldsymbol{q} \in \boldsymbol{P}_{k-1}(e),\ \forall e \in \mathcal{E}_h^i\right\}.$$

Let O be an 1 or 2 dimensional geometrical object (edge or polygon). For an integer $k \geq 0$, $P_k(O)$ denotes the space of polynomials of degree $\leq k$ on O. $M_k(O)$ denotes the set of scaled monomials of degree $\leq k$ on O, that is,

$$M_k(O) = \left\{\left(\frac{\boldsymbol{x} - \boldsymbol{x}_O}{h_O}\right)^{\boldsymbol{\alpha}} : |\boldsymbol{\alpha}| \leq k\right\},$$

where $\boldsymbol{x}$ is a local coordinate system on O, $\boldsymbol{x}_O$ is the barycenter of O in the local coordinate system, $\boldsymbol{\alpha}$ is a multi-index, and $h_O = \mathrm{diam}(O)$.

Conventionally we define $P_{-1}(O) = \{0\}$. We also define $\boldsymbol{P}_k(O) = (P_k(O))^2$ for $k \geq -1$ and $\boldsymbol{M}_k(O) = (M_k(O))^2$ for any nonnegative integer k.

Let $K \in \mathcal{P}_h$ and let k be a nonnegative integer. We define $(\nabla P_{k+1}(K))^{\oplus}$ as the subspace of $\boldsymbol{P}_k(K)$ satisfying

$$\boldsymbol{P}_k(K) = \nabla P_{k+1}(K) \oplus (\nabla P_{k+1}(K))^{\oplus},$$

and denote by $\boldsymbol{M}_k^{\oplus}$ a basis of the space $(\nabla P_{k+1}(K))^{\oplus}$. For example, one can choose

$$(\nabla P_{k+1}(K))^{\oplus} = \boldsymbol{x}^{\perp} P_{k-1}(K), \quad \boldsymbol{M}_k^{\oplus} = \{m(\boldsymbol{x})\boldsymbol{x}^{\perp} : m \in M_{k-1}(K)\},$$

where $\boldsymbol{x}^{\perp} = (x_2, -x_1)$ with $\boldsymbol{x} = (x_1, x_2)$.

3.2 Virtual element space

We first define a local virtual element space on each element $K \in \mathcal{P}_h$. Let k be a fixed positive integer. Let

$$\boldsymbol{W}_h^1(K) := \{\boldsymbol{v} \in \boldsymbol{H}^1(K) : \operatorname{div} \boldsymbol{v} \in P_{k-1}(K),\ \operatorname{rot} \boldsymbol{v} = 0,\ \boldsymbol{v}\cdot\boldsymbol{n}_K|_e \in P_k(e),\ \forall e \subset \partial K\},$$

where $\operatorname{rot} \boldsymbol{v} = \frac{\partial v_1}{\partial x_2} - \frac{\partial v_2}{\partial x_1}$ for $\boldsymbol{v} = (v_1, v_2) \in \boldsymbol{H}^1(K)$. Also, let

$$\Phi_h(K) := \{\phi \in H^2(K) : \Delta^2\phi \in P_{k-3}(K),\ \phi|_e = 0,\ \Delta\phi|_e \in P_{k-1}(e),\ \forall e \subset \partial K\}$$

with the convention that $P_{-1}(K) = P_{-2}(K) = \{0\}$. In [29, Lemma 2], it was shown that $\boldsymbol{W}_h^1(K) \cap \operatorname{\mathbf{curl}} \Phi_h(K) = \{0\}$, where $\operatorname{\mathbf{curl}} q = \left(-\frac{\partial q}{\partial x_2}, \frac{\partial q}{\partial x_1}\right)$ for $q \in H^1(K)$. It was also shown in [29, Lemma 3] that if the local space $\tilde{\boldsymbol{V}}_h(K)$ is defined by

$$\tilde{\boldsymbol{V}}_h(K) = \boldsymbol{W}_h^1(K) \oplus \operatorname{\mathbf{curl}} \Phi_h(K),$$

then the following degrees of freedom (DOFs) are unisolvent for $\tilde{\boldsymbol{V}}_h(K)$:

$$\begin{aligned}
&\text{the moments } \frac{1}{|e|}\int_e \boldsymbol{v}\cdot\boldsymbol{n}_e q \,\mathrm{d}s, && q \in M_k(e),\\
&\text{the moments } \frac{1}{|e|}\int_e \boldsymbol{v}\cdot\boldsymbol{t}_e q \,\mathrm{d}s, && q \in M_{k-1}(e),\\
&\text{the moments } \frac{1}{|K|}\int_K \boldsymbol{v}\cdot\boldsymbol{q} \,\mathrm{d}\boldsymbol{x}, && \boldsymbol{q} \in \boldsymbol{M}_{k-2}(K).
\end{aligned}$$

We define a local projection $\Pi_K^\nabla : \boldsymbol{H}^1(K) \to \boldsymbol{P}_k(K)$ on each polygon K in $\mathcal{P}_h$. It is defined by

$$\begin{aligned}
\int_K \nabla(\Pi_K^\nabla \boldsymbol{v}) : \nabla \boldsymbol{q} \,\mathrm{d}\boldsymbol{x} &= \int_K \nabla \boldsymbol{v} : \nabla \boldsymbol{q} \,\mathrm{d}\boldsymbol{x}, \quad \forall \boldsymbol{v} \in \boldsymbol{H}^1(K),\ \forall \boldsymbol{q} \in \boldsymbol{P}_k(K),\\
\int_{\partial K} \Pi_K^\nabla \boldsymbol{v} \,\mathrm{d}s &= \int_{\partial K} \boldsymbol{v} \,\mathrm{d}s,
\end{aligned}$$

for $\boldsymbol{v} \in \boldsymbol{H}^1(K)$. Note that $\Pi_K^\nabla \boldsymbol{q} = \boldsymbol{q}$ for any $\boldsymbol{q} \in \boldsymbol{P}_k(K)$ and the local projection Π_K^∇ is computable using only the moments of $\boldsymbol{v}$ up to order $(k-1)$ on each edge $e \subset \partial K$ and the moments of $\boldsymbol{v}$ up to order $(k-2)$ on K.

Now the local nonconforming virtual element space $\boldsymbol{V}_h(K)$ on K is defined by

$$\boldsymbol{V}_h(K) = \left\{ \boldsymbol{v} \in \tilde{\boldsymbol{V}}_h(K) : \int_e (\boldsymbol{v} - \Pi_K^\nabla \boldsymbol{v})\cdot\boldsymbol{n}_e q \,\mathrm{d}s = 0,\ \forall q \in P_k(e)/P_{k-1}(e),\ \forall e \subset \partial K \right\},$$

where $P_k(e)/P_{k-1}(e)$ is the subspace of polynomials in $P_k(e)$ that are $L^2(e)$-orthogonal to $P_{k-1}(e)$. It was shown in [29] that the following DOFs are unisolvent for $\boldsymbol{V}_h(K)$:

$$\frac{1}{|e|}\int_e \boldsymbol{v}\cdot\boldsymbol{n}_e q\,\mathrm{d}s, \qquad q\in M_{k-1}(e),$$
$$\frac{1}{|e|}\int_e \boldsymbol{v}\cdot\boldsymbol{t}_e q\,\mathrm{d}s, \qquad q\in M_{k-1}(e),$$
$$\frac{1}{|K|}\int_K \boldsymbol{v}\cdot\boldsymbol{q}\,\mathrm{d}\boldsymbol{x}, \qquad \boldsymbol{q}\in \boldsymbol{M}_{k-2}(K).$$

For each $i = 1, 2, \cdots, N_K := \dim \boldsymbol{V}_h(K)$, let χ_i be the operator associated to the ith local DOF. Then, for any $\boldsymbol{v}\in \boldsymbol{H}^1(K)$, there exists a unique element $I_h^K\boldsymbol{v}\in \boldsymbol{V}_h(K)$ such that

$$\chi_i(\boldsymbol{v}-I_h^K\boldsymbol{v}) = 0 \quad \forall i = 1, 2, \cdots, N_K.$$

The operator $\boldsymbol{v}\mapsto I_h^K\boldsymbol{v}$ is called a local interpolation operator for $\boldsymbol{V}_h(K)$. It was shown in [29] that we can obtain the following interpolation error estimates.

Proposition 1 (see [29, Lemma 6]) *There exists a positive constant C independent of h such that for every $K\in\mathcal{P}_h$ and every $\boldsymbol{v}\in \boldsymbol{H}^s(K)$ with $1\le s\le k+1$,*

$$\|\boldsymbol{v}-I_h^K\boldsymbol{v}\|_{0,K} + h|\boldsymbol{v}-I_h^K\boldsymbol{v}|_{1,K} \le Ch^s|\boldsymbol{v}|_{s,K}.$$

The global nonconforming virtual element spaces are defined as follows:

$$\boldsymbol{V}_h = \Big\{\boldsymbol{v}_h\in \boldsymbol{L}^2(\Omega)\ :\ \boldsymbol{v}_h|_K\in \boldsymbol{V}_h(K) \quad \forall K\in\mathcal{P}_h,$$
$$\int_e [\boldsymbol{v}_h]_e\cdot\boldsymbol{q}\,\mathrm{d}s = 0 \quad \forall \boldsymbol{q}\in \boldsymbol{P}_{k-1}(e),\ \forall e\in\mathcal{E}_h^i\Big\},$$
$$\boldsymbol{V}_{h,0} = \Big\{\boldsymbol{v}_h\in \boldsymbol{L}^2(\Omega)\ :\ \boldsymbol{v}_h|_K\in \boldsymbol{V}_h(K) \quad \forall K\in\mathcal{P}_h,$$
$$\int_e [\boldsymbol{v}_h]_e\cdot\boldsymbol{q}\,\mathrm{d}s = 0 \quad \forall \boldsymbol{q}\in \boldsymbol{P}_{k-1}(e),\ \forall e\in\mathcal{E}_h\Big\}.$$

The global DOFs for $\boldsymbol{V}_h$ can be chosen as, for any edge e and polygon K in $\mathcal{P}_h$,

$$\chi_{e,q}^n(\boldsymbol{v}_h) := \frac{1}{|e|}\int_e \boldsymbol{v}_h\cdot\boldsymbol{n}_e q\,\mathrm{d}s, \qquad q\in M_{k-1}(e), \tag{5}$$
$$\chi_{e,q}^t(\boldsymbol{v}_h) := \frac{1}{|e|}\int_e \boldsymbol{v}_h\cdot\boldsymbol{t}_e q\,\mathrm{d}s, \qquad q\in M_{k-1}(e), \tag{6}$$
$$\chi_{K,\boldsymbol{q}}(\boldsymbol{v}_h) := \frac{1}{|K|}\int_K \boldsymbol{v}_h\cdot\boldsymbol{q}\,\mathrm{d}\boldsymbol{x}, \qquad \boldsymbol{q}\in \nabla M_{k-1}(K) + \boldsymbol{M}_{k-2}^{\oplus}(K). \tag{7}$$

Similarly, the global DOFs for $\boldsymbol{V}_{h,0}$ can be chosen. We also define the global interpolation operator $I_h : \boldsymbol{H}^{1,nc}(\Omega;\mathcal{P}_h)\to \boldsymbol{V}_h$ by $(I_h\boldsymbol{v})|_K = I_h^K(\boldsymbol{v}|_K)$ for each $K\in\mathcal{P}_h$ and $\boldsymbol{v}\in \boldsymbol{H}^{1,nc}(\Omega;\mathcal{P}_h)$.

The discrete pressure space Q_h is defined by

$$Q_h = \{q_h\in L_0^2(\Omega) : q_h|_K\in P_{k-1}(K)\ \forall K\in\mathcal{P}_h\}.$$

The global DOFs for the space Q_h can be chosen as

$$\frac{1}{|K|}\int_K q_h\phi \mathrm{d}\boldsymbol{x}, \quad \phi \in M_{k-1}(K),\ K \in \mathcal{P}_h.$$

It was shown in [29] that div $\boldsymbol{V}_h(K) \subset P_{k-1}(K)$ for each $K \in \mathcal{P}_h$, and $\mathrm{div}_h \boldsymbol{V}_{h,0} \subset Q_h$, where div_h denotes the discrete divergence operator defined by $(\mathrm{div}_h \boldsymbol{v}_h)|_K = \mathrm{div}(\boldsymbol{v}_h|_K)$ for each $K \in \mathcal{P}_h$ and $\boldsymbol{v}_h \in \boldsymbol{V}_h$. Therefore, the nonconforming virtual element space $\boldsymbol{V}_h$ is divergence-free.

3.3 The discrete problem

We define a local discrete bilinear form a_h^K for each polygon K in $\mathcal{P}_h$, as follows.

$$\begin{aligned} a_h^K(\boldsymbol{v}_h, \boldsymbol{w}_h) = {} & a^K(\Pi_K^\nabla(\boldsymbol{v}_h), \Pi_K^\nabla(\boldsymbol{w}_h)) \\ & + S^K((I-\Pi_K^\nabla)\boldsymbol{v}_h, (I-\Pi_K^\nabla)\boldsymbol{w}_h), \quad \boldsymbol{v}_h, \boldsymbol{w}_h \in \boldsymbol{V}_h(K), \end{aligned}$$

where a^K is the bilinear form defined by

$$a^K(\boldsymbol{v}, \boldsymbol{w}) = \int_K \nabla \boldsymbol{v} : \nabla \boldsymbol{w} \mathrm{d}\boldsymbol{x}, \quad \boldsymbol{v}, \boldsymbol{w} \in \boldsymbol{H}^1(K),$$

and S^K is a symmetric positive definite bilinear form defined as

$$S^K(\boldsymbol{v}_h, \boldsymbol{w}_h) = \sum_{i=1}^{N_K} \chi_i(\boldsymbol{v}_h)\chi_i(\boldsymbol{w}_h), \quad \boldsymbol{v}_h, \boldsymbol{w}_h \in \boldsymbol{V}_h(K),$$

where $N_K = \dim(\boldsymbol{V}_h(K))$ and χ_i denotes the operator associated to the ith local DOF for $i = 1, 2, \cdots, N_K$. As described in [5, 29], we obtain the k-consistency and stability of a_h^K:

- (k-consistency) $a_h^K(\boldsymbol{q}, \boldsymbol{v}_h) = a^K(\boldsymbol{q}, \boldsymbol{v}_h)$ for any $\boldsymbol{q} \in \boldsymbol{P}_k(K)$, $\boldsymbol{v}_h \in \boldsymbol{V}_h(K)$;
- (stability) there exist constants $c_*, c^* > 0$ independent of h such that

$$c_* a^K(\boldsymbol{v}_h, \boldsymbol{v}_h) \le a_h^K(\boldsymbol{v}_h, \boldsymbol{v}_h) \le c^* a^K(\boldsymbol{v}_h, \boldsymbol{v}_h) \quad \forall \boldsymbol{v}_h \in \boldsymbol{V}_h(K).$$

The global bilinear form a_h is defined by

$$a_h(\boldsymbol{v}_h, \boldsymbol{w}_h) = \sum_{K \in \mathcal{P}_h} a_h^K(\boldsymbol{v}_h, \boldsymbol{w}_h), \quad \boldsymbol{v}_h, \boldsymbol{w}_h \in \boldsymbol{V}_h.$$

On the other hand, the discrete bilinear form b_h is simply defined by

$$b_h(\boldsymbol{v}_h, q_h) = \sum_{K \in \mathcal{P}_h} b^K(\boldsymbol{v}_h, q_h), \quad \boldsymbol{v}_h \in \boldsymbol{V}_h,\ q_h \in Q_h,$$

where

$$b^K(\boldsymbol{v}, q) = -\int_K q \ \mathrm{div}\ \boldsymbol{v} \mathrm{d}\boldsymbol{x},$$

for $\boldsymbol{v} \in \boldsymbol{H}^1(K)$, $q \in P_{k-1}(K)$, and $K \in \mathcal{P}_h$. Note that $b_h(\boldsymbol{v}_h, q_h)$ is also computable using only the DOFs (5)–(7) and we do not rely on the discrete version of it, indeed we omit the subscript h on such bilinear form.

We next discretize the right-hand side $(\boldsymbol{f}, \cdot)_{0,\Omega}$ as follows:

$$\langle \boldsymbol{f}_h, \boldsymbol{v}_h \rangle = \begin{cases} (\boldsymbol{f}_h, \overline{\boldsymbol{v}}_h)_{0,\Omega} & \text{if } k = 1 \\ (\boldsymbol{f}_h, \boldsymbol{v}_h)_{0,\Omega} & \text{if } k > 1 \end{cases}, \quad \boldsymbol{v}_h \in \boldsymbol{V}_h,$$

where $\boldsymbol{f}_h, \overline{\boldsymbol{v}}_h \in \boldsymbol{L}^2(\Omega)$ are defined by

$$\boldsymbol{f}_h|_K = \begin{cases} \Pi_0^K \boldsymbol{f} & \text{if } k = 1 \\ \Pi_{k-2}^K \boldsymbol{f} & \text{if } k > 1 \end{cases}, \quad \overline{\boldsymbol{v}}_h|_K = \frac{1}{|\partial K|} \int_{\partial K} \boldsymbol{v}_h \mathrm{d}s, \quad K \in \mathcal{P}_h.$$

Here, Π_ℓ^K denotes the L^2-projection operator onto $\boldsymbol{P}_\ell(K)$ for each $K \in \mathcal{P}_h$.

In order to consider the nonhomogeneous Dirichlet boundary condition, let

$$\boldsymbol{V}_{h,\boldsymbol{g}} = \left\{ \boldsymbol{v}_h \in \boldsymbol{V}_h : \int_e \boldsymbol{g} \cdot \boldsymbol{q} \mathrm{d}s = \int_e \boldsymbol{v}_h \cdot \boldsymbol{q} \mathrm{d}s, \ \forall \boldsymbol{q} \in \boldsymbol{P}_{k-1}(e), \ \forall e \in \mathcal{E}_h^\partial \right\}.$$

We formulate the nonconforming VEM for the Stokes problem (3) as follows: Find $\boldsymbol{u}_h \in \boldsymbol{V}_{h,\boldsymbol{g}}$ and $p_h \in Q_h$ such that

$$\begin{cases} a_h(\boldsymbol{u}_h, \boldsymbol{v}_h) + b_h(\boldsymbol{v}_h, p_h) & = & \langle \boldsymbol{f}_h, \boldsymbol{v}_h \rangle & \forall \boldsymbol{v}_h \in \boldsymbol{V}_{h,0}, \\ b_h(\boldsymbol{u}_h, q_h) & = & 0 & \forall q_h \in Q_h. \end{cases} \tag{8}$$

Here $\boldsymbol{u}_h$ and p_h will be called discrete velocity and discrete pressure, respectively. It was shown in [29] that the bilinear form $b_h(\cdot, \cdot)$ satisfies the inf-sup condition and the discrete problem (8) is well-posed. Moreover, for the case $\boldsymbol{g} = \boldsymbol{0}$, we can obtain the following error estimate.

Theorem 1 (see [29, Theorem 13]) *Suppose that $\boldsymbol{f} \in \boldsymbol{H}^{k-1}(\Omega)$ and $\boldsymbol{g} = \boldsymbol{0}$. Let $(\boldsymbol{u}, p) \in (\boldsymbol{H}_0^1(\Omega) \cap \boldsymbol{H}^{k+1}(\Omega)) \times (L_0^2(\Omega) \cap H^k(\Omega))$ be the solution of the continuous problem (3). Let $(\boldsymbol{u}_h, p_h) \in \boldsymbol{V}_{h,0} \times Q_h$ be the solution of the discrete problem (8). Then,*

$$|\boldsymbol{u} - \boldsymbol{u}_h|_{1,h} + \|p - p_h\|_{0,\Omega} \leq Ch^k (|\boldsymbol{u}|_{k+1,\Omega} + |p|_{k,\Omega} + |\boldsymbol{f}|_{k-1,\Omega}),$$

where C is a positive constant independent on h.

4 A formal construction of divergence-free basis

In this section, we present a formal construction of a divergence-free basis for the virtual element space $\boldsymbol{V}_{h,0}$.

We first define the canonical basis associated with the DOFs (5)–(7) of the space $\boldsymbol{V}_h$. Recall that the global DOFs of $\boldsymbol{V}_h$ are given by

$$\chi_{e,q}^n(\boldsymbol{v}_h) = \frac{1}{|e|} \int_e \boldsymbol{v}_h \cdot \boldsymbol{n}_e q \mathrm{d}s, \qquad q \in M_{k-1}(e), \ e \in \mathcal{E}_h,$$

$$\chi_{e,q}^t(\boldsymbol{v}_h) = \frac{1}{|e|} \int_e \boldsymbol{v}_h \cdot \boldsymbol{t}_e q \mathrm{d}s, \qquad q \in M_{k-1}(e), \ e \in \mathcal{E}_h,$$

$$\chi_{K,\boldsymbol{q}}(\boldsymbol{v}_h) = \frac{1}{|K|} \int_K \boldsymbol{v}_h \cdot \boldsymbol{q} \mathrm{d}\boldsymbol{x}, \qquad \boldsymbol{q} \in \nabla M_{k-1}(K) + \boldsymbol{M}_{k-2}^{\oplus}(K), \ K \in \mathcal{P}_h.$$

We sometimes write χ to denote $\chi^n_{e,q}$, $\chi^t_{e,q}$, or $\chi_{K,\boldsymbol{q}}$ when it is clear from the context. Using these notations, we define the canonical basis functions of $\boldsymbol{V}_h$ associated to the DOFs (5)–(7) as follows:

- For $e \in \mathcal{E}_h$ and $q \in M_{k-1}(e)$, let $\boldsymbol{\varphi}^n_{e,q}$ be the function in $\boldsymbol{V}_h$ such that $\chi^n_{e,q}(\boldsymbol{\varphi}^n_{e,q}) = 1$ and $\chi(\boldsymbol{\varphi}^n_{e,q}) = 0$ for all other DOFs.
- For $e \in \mathcal{E}_h$ and $q \in M_{k-1}(e)$, let $\boldsymbol{\varphi}^t_{e,q}$ be the function in $\boldsymbol{V}_h$ such that $\chi^t_{e,q}(\boldsymbol{\varphi}^t_{e,q}) = 1$ and $\chi(\boldsymbol{\varphi}^t_{e,q}) = 0$ for all other DOFs.
- For $K \in \mathcal{P}_h$ and $\boldsymbol{q} \in (\nabla M_{k-1}(K)) + \boldsymbol{M}^{\oplus}_{k-2}(K)$, let $\boldsymbol{\varphi}_{K,\boldsymbol{q}}$ be the function in $\boldsymbol{V}_h$ such that $\chi_{K,\boldsymbol{q}}(\boldsymbol{\varphi}_{K,\boldsymbol{q}}) = 1$ and $\chi = 0$ for all other DOFs.

Let us define

$$\boldsymbol{Z}_h = \{\boldsymbol{v}_h \in \boldsymbol{V}_h : \mathrm{div}_h \boldsymbol{v}_h = 0\}, \quad \boldsymbol{Z}_{h,0} = \{\boldsymbol{v}_h \in \boldsymbol{V}_{h,0} : \mathrm{div}_h \boldsymbol{v}_h = 0\}.$$

We first compute the dimension of $\boldsymbol{Z}_{h,0}$.

Proposition 2 *The dimension of $\boldsymbol{Z}_{h,0}$ is*

$$N_{V,i} + kN_{E,i} + (k-1)N_{E,i} + \frac{(k-1)(k-2)}{2} N_P.$$

Proof Since $\mathrm{div}_h \boldsymbol{V}_{h,0} = Q_h$ and since $\mathrm{div}_h \boldsymbol{V}_{h,0} \cong \boldsymbol{V}_{h,0}/\boldsymbol{Z}_{h,0}$, we obtain

$$\dim \boldsymbol{Z}_{h,0} = \dim \boldsymbol{V}_{h,0} - \dim(\mathrm{div}_h \boldsymbol{V}_{h,0}) = \dim \boldsymbol{V}_{h,0} - \dim Q_h.$$

Note that

$$\dim \boldsymbol{V}_{h,0} = 2\left(\frac{k(k-1)}{2} N_P + kN_{E,i}\right), \quad \dim Q_h = \frac{k(k+1)}{2} N_P - 1,$$

Since $N_P - N_{E,i} + N_{V,i} = 1$ from Euler's formula, we have

$$\begin{aligned}
\dim \boldsymbol{Z}_{h,0} &= \dim \boldsymbol{V}_{h,0} - \dim Q_h = k(k-1)N_P + 2kN_{E,i} - \frac{k(k+1)}{2} N_P + 1 \\
&= k(k-1)N_P + 2kN_{E,i} - \frac{k(k+1)}{2} N_P + N_P - N_{E,i} + N_{V,i} \\
&= N_{V,i} + kN_{E,i} + (k-1)N_{E,i} + \frac{(k-1)(k-2)}{2} N_P.
\end{aligned}$$

This concludes the proof of the proposition. □

In order to construct a basis of $\boldsymbol{Z}_{h,0}$, we first define some functions in $\boldsymbol{V}_h$.

(D1) For each vertex $v \in \mathcal{V}_h$, let $e_1, \cdots, e_l$ be the edges in $\mathcal{E}_h$ having v as an end point, and let $K_1, \cdots, K_l$ be the elements in $\mathcal{P}_h$ having v as a vertex. For each $i = 1, \cdots, l$, let $\boldsymbol{n}_{e_i,v}$ be a unit vector normal to e_i pointing in the counterclockwise direction with respect to the vertex v (see Fig. 1a). Define $\boldsymbol{\psi}_v \in \boldsymbol{V}_h$ by

$$\boldsymbol{\psi}_v := h \sum_{i=1}^{l} \frac{\langle \boldsymbol{n}_{e_i}, \boldsymbol{n}_{e_i,v} \rangle}{|e_i|} \boldsymbol{\varphi}^n_{e_i,1} + \sum_{j=1}^{l} \sum_{q \in M_{k-1}(K_j) \setminus \{1\}} c_{j,q} \boldsymbol{\varphi}_{K_j,\nabla q},$$

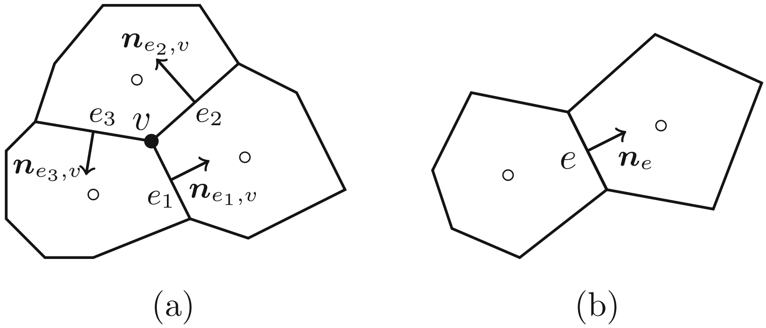

Fig. 1 Examples of functions defined in (D1) (**a**) and (D3) (**b**)

where

$$c_{j,q} = \frac{h}{|K_j|} \sum_{i=1}^{l} \frac{\langle \boldsymbol{n}_{e_i}, \boldsymbol{n}_{e_i,v} \rangle}{|e_i|} \int_{e_i \cap \partial K_j} \boldsymbol{\varphi}^n_{e_i,1} \cdot \boldsymbol{n}_{K_j} q \mathrm{d}s$$

for $q \in M_{k-1}(K_j) \setminus \{1\}$ and $j = 1, \cdots, l$.

(D2) For each edge $e \in \mathcal{E}_h$ and each $q \in M_{k-1}(e)$, define $\boldsymbol{\psi}^t_{e,q}$ by

$$\boldsymbol{\psi}^t_{e,q} = \boldsymbol{\varphi}^t_{e,q}.$$

(D3) Assume $k \geq 2$. For each edge $e \in \mathcal{E}_h$ and each $q \in M_{k-1}(e) \setminus \{1\}$, define $\boldsymbol{\psi}^n_{e,q}$ by

$$\boldsymbol{\psi}^n_{e,q} = \boldsymbol{\varphi}^n_{e,q} + \sum_{K \in \mathcal{P}_h} \sum_{r \in M_{k-1}(K) \setminus \{1\}} c_{K,r} \boldsymbol{\varphi}_{K,\nabla r},$$

where

$$c_{K,r} = \frac{1}{|K|} \int_{e \cap \partial K} \boldsymbol{\varphi}^n_{e,q} \cdot \boldsymbol{n}_K r \mathrm{d}s, \quad r \in M_{k-1}(K) \setminus \{1\}, \ K \in \mathcal{P}_h.$$

(See Fig. 1b.)

(D4) Assume $k \geq 3$. For each $K \in \mathcal{P}_h$ and each $\boldsymbol{q} \in \boldsymbol{M}^{\oplus}_k$, define $\boldsymbol{\psi}_{K,\boldsymbol{q}}$ by

$$\boldsymbol{\psi}_{K,\boldsymbol{q}} = \boldsymbol{\varphi}_{K,\boldsymbol{q}}.$$

Remark 1 The coefficients $c_{j,q}$ and $c_{K,r}$ defined in (D1) and (D3) are exactly computable using the DOFs (5)–(7). Moreover, since it is computed elementwise, the cost of computing the coefficients is negligible.

We first show that the functions defined in (D1)–(D4) are indeed contained in $\boldsymbol{Z}_h$.

Lemma 1 *The functions defined in (D1)–(D4) are contained in* $\mathbf{Z}_h$.

Proof Since div $\boldsymbol{V}_h(K) \subset P_{k-1}(K)$ for each $K \in \mathcal{P}_h$, if $\boldsymbol{v}_h \in \boldsymbol{V}_h$, then

$$\boldsymbol{v}_h \in \boldsymbol{Z}_h \quad \text{if and only if} \quad \int_K q \operatorname{div} \boldsymbol{v}_h \mathrm{d}\boldsymbol{x} = 0 \ \forall q \in M_{k-1}(K), \ \forall K \in \mathcal{P}_h. \tag{9}$$

From (9), the functions in (D2) and (D4) are obviously contained in $\boldsymbol{Z}_h$. We first show that the functions in (D1) belong to $\boldsymbol{Z}_h$. Note that

$$\int_K q \operatorname{div} \boldsymbol{\psi}_v \mathrm{d}\boldsymbol{x} = 0 \quad \forall q \in M_{k-1}(K),\ \forall K \in \mathcal{P}_h \text{ with } K \neq K_1, \cdots, K_l.$$

Let $j = 1, \cdots, l$. Since K_j is a polygon having v as a vertex, there are exactly two edges $e_{i_1,v}$ and $e_{i_2,v}$ with $1 \leq i_1, i_2 \leq l$ such that $e_{i_1,v}, e_{i_2,v} \subset \partial K_j$. Moreover, one of the normal vectors $\boldsymbol{n}_{e_1,v}$ and $\boldsymbol{n}_{e_2,v}$ coincides with $\boldsymbol{n}_{K_j}$, and the other has the opposite direction of $\boldsymbol{n}_{K_j}$. We may assume that $\boldsymbol{n}_{e_{i_1,v}} = \boldsymbol{n}_{K_j}|_{e_{i_1}}$ and $\boldsymbol{n}_{e_{i_2,v}} = -\boldsymbol{n}_{K_j}|_{e_{i_2}}$. Then,

$$\begin{aligned}
\int_{K_j} \operatorname{div} \boldsymbol{\psi}_v \mathrm{d}\boldsymbol{x} &= \int_{\partial K_j} \boldsymbol{\psi}_v \cdot \boldsymbol{n}_{K_j} \mathrm{d}s \\
&= h \frac{\langle \boldsymbol{n}_{e_{i_1}}, \boldsymbol{n}_{e_{i_1,v}} \rangle}{|e_{i_1}|} \int_{e_{i_1}} \boldsymbol{\varphi}^n_{e_{i_1},1} \cdot \boldsymbol{n}_{K_j}|_{e_{i_1}} \mathrm{d}s + h \frac{\langle \boldsymbol{n}_{e_{i_2}}, \boldsymbol{n}_{e_{i_2,v}} \rangle}{|e_{i_2}|} \int_{e_{i_2}} \boldsymbol{\varphi}^n_{e_{i_2},1} \cdot \boldsymbol{n}_{K_j}|_{e_{i_2}} \mathrm{d}s \\
&= h \langle \boldsymbol{n}_{e_{i_1}}, \boldsymbol{n}_{e_{i_1,v}} \rangle \langle \boldsymbol{n}_{K_j}|_{e_{i_1}}, \boldsymbol{n}_{e_{i_1}} \rangle + h \langle \boldsymbol{n}_{e_{i_2}}, \boldsymbol{n}_{e_{i_2,v}} \rangle \langle \boldsymbol{n}_{K_j}|_{e_{i_2}}, \boldsymbol{n}_{e_{i_2}} \rangle \\
&= h \langle \boldsymbol{n}_{e_{i_1}}, \boldsymbol{n}_{e_{i_1,v}} \rangle \langle \boldsymbol{n}_{e_{i_1,v}}, \boldsymbol{n}_{e_{i_1}} \rangle - h \langle \boldsymbol{n}_{e_{i_2}}, \boldsymbol{n}_{e_{i_2,v}} \rangle \langle \boldsymbol{n}_{e_{i_2,v}}, \boldsymbol{n}_{e_{i_2}} \rangle \\
&= 0.
\end{aligned}$$

Suppose $q \in M_{k-1}(K_j) \setminus \{1\}$. Then,

$$\begin{aligned}
\int_{K_j} q \operatorname{div} \boldsymbol{\psi}_v \mathrm{d}\boldsymbol{x} &= \int_{\partial K_j} q \boldsymbol{\psi}_v \cdot \boldsymbol{n}_K \mathrm{d}s - \int_{K_j} \boldsymbol{\psi}_v \cdot \nabla q \mathrm{d}\boldsymbol{x} \\
&= h \sum_{i=1}^{l} \frac{\langle \boldsymbol{n}_{e_i}, \boldsymbol{n}_{e_i,v} \rangle}{|e_i|} \int_{e_i \cap \partial K_j} q \boldsymbol{\varphi}^n_{e_i,1} \cdot \boldsymbol{n}_{K_j} \mathrm{d}s \\
&\quad - \sum_{q' \in M_{k-1}(K_j) \setminus \{1\}} c_{j,q'} \int_{K_j} \boldsymbol{\varphi}_{K_j, \nabla q'} \cdot \nabla q \mathrm{d}\boldsymbol{x} \\
&= h \sum_{i=1}^{l} \frac{\langle \boldsymbol{n}_{e_i}, \boldsymbol{n}_{e_i,v} \rangle}{|e_i|} \int_{e_i \cap \partial K_j} q \boldsymbol{\varphi}^n_{e_i,1} \cdot \boldsymbol{n}_{K_j} \mathrm{d}s - c_{j,q} \int_{K_j} \boldsymbol{\varphi}_{K_j, \nabla q} \cdot \nabla q \mathrm{d}\boldsymbol{x} \\
&= h \sum_{i=1}^{l} \frac{\langle \boldsymbol{n}_{e_i}, \boldsymbol{n}_{e_i,v} \rangle}{|e_i|} \int_{e_i \cap \partial K_j} q \boldsymbol{\varphi}^n_{e_i,1} \cdot \boldsymbol{n}_{K_j} \mathrm{d}s - |K_j| c_{j,q} \\
&= 0.
\end{aligned}$$

Here we used the relations

$$\int_{K_j} \boldsymbol{\varphi}_{K_j, \nabla q'} \cdot \nabla q \mathrm{d}\boldsymbol{x} = \begin{cases} |K_j| & \text{if } q = q' \\ 0 & \text{if } q \neq q'. \end{cases}$$

Thus, $\boldsymbol{\psi}_v \in \boldsymbol{Z}_h$. We next show that the functions $\boldsymbol{\psi}^n_{e,q}$ in (D3) belong to $\boldsymbol{Z}_h$. Note that $c_{K,r} = 0$ for any $r \in M_{k-1}(K) \setminus \{1\}$ and any $K \in \mathcal{P}_h$ with $e \not\subset \partial K$. Then,

$$\begin{aligned}
\int_K r \operatorname{div} \boldsymbol{\psi}^n_{e,q} \mathrm{d}\boldsymbol{x} &= \int_{\partial K} r \boldsymbol{\psi}^n_{e,q} \cdot \boldsymbol{n}_K \mathrm{d}s - \int_K \boldsymbol{\psi}^n_{e,q} \cdot \nabla r \mathrm{d}\boldsymbol{x} \\
&= \int_{\partial K} r \boldsymbol{\psi}^n_{e,q} \cdot \boldsymbol{n}_K \mathrm{d}s = 0
\end{aligned}$$

for any $r \in M_{k-1}(K) \setminus \{1\}$ and $K \in \mathcal{P}_h$ with $e \not\subset \partial K$. We next suppose that $K \in \mathcal{P}_h$ satisfies $e \subset \partial K$. Since $q \neq 1$,

$$\int_K \operatorname{div} \boldsymbol{\psi}_{e,q}^n \mathrm{d}\boldsymbol{x} = \int_{\partial K} \boldsymbol{\psi}_{e,q}^n \cdot \boldsymbol{n}_K \mathrm{d}s = 0,$$

and

$$\begin{aligned}
\int_K r \operatorname{div} \boldsymbol{\psi}_{e,q}^n \mathrm{d}\boldsymbol{x} &= \int_{\partial K} r \boldsymbol{\psi}_{e,q}^n \cdot \boldsymbol{n}_K \mathrm{d}s - \int_K \boldsymbol{\psi}_{e,q}^n \cdot \nabla r \mathrm{d}\boldsymbol{x} \\
&= \int_{e \cap \partial K} r \boldsymbol{\varphi}_{e,q}^n \cdot \boldsymbol{n}_K \mathrm{d}s - \sum_{r' \in M_{k-1}(K) \setminus \{1\}} c_{K,r'} \int_K \boldsymbol{\varphi}_{K,\nabla r'} \cdot \nabla r \mathrm{d}\boldsymbol{x} \\
&= \int_{e \cap \partial K} r \boldsymbol{\varphi}_{e,q}^n \cdot \boldsymbol{n}_K \mathrm{d}s - c_{K,r} \int_K \boldsymbol{\varphi}_{K,\nabla r} \cdot \nabla r \mathrm{d}\boldsymbol{x} \\
&= \int_{e \cap \partial K} r \boldsymbol{\varphi}_{e,q}^n \cdot \boldsymbol{n}_K \mathrm{d}s - |K| c_{K,r} = 0
\end{aligned}$$

for any $r \in M_{k-1}(K) \setminus \{1\}$. Here, as before, we used the relations

$$\int_K \boldsymbol{\varphi}_{K,\nabla r'} \cdot \nabla r \mathrm{d}\boldsymbol{x} = \begin{cases} |K| & \text{if } r = r' \\ 0 & \text{if } r \neq r'. \end{cases}$$

Thus, $\boldsymbol{\psi}_{e,q}^n \in \boldsymbol{Z}_h$. This concludes the proof of the lemma. □

The next theorem shows that some of these functions generate a basis for $\boldsymbol{Z}_{h,0}$.

Theorem 2 *Let $\boldsymbol{Z}_1, \boldsymbol{Z}_2, \boldsymbol{Z}_3, \boldsymbol{Z}_4$ be the subspaces of $\mathbf{V}_h$ defined by*

$$\begin{aligned}
\boldsymbol{Z}_1 &= \operatorname{span}(\{\boldsymbol{\psi}_v : v \in \mathcal{V}_h^i\}), \\
\boldsymbol{Z}_2 &= \operatorname{span}(\{\boldsymbol{\psi}_{e,q}^t : q \in M_{k-1}(e), e \in \mathcal{E}_h^i\}), \\
\boldsymbol{Z}_3 &= \begin{cases} \operatorname{span}(\{\boldsymbol{\psi}_{e,q}^n : q \in M_{k-1}(e) \setminus \{1\}, e \in \mathcal{E}_h^i\}) & \text{if } k \geq 2 \\ \{0\} & \text{otherwise} \end{cases}, \\
\boldsymbol{Z}_4 &= \begin{cases} \operatorname{span}(\{\boldsymbol{\psi}_{K,\boldsymbol{q}} : \boldsymbol{q} \in \boldsymbol{M}_k^{\oplus}, K \in \mathcal{P}_h\}) & \text{if } k \geq 3 \\ \{0\} & \text{otherwise} \end{cases},
\end{aligned}$$

where $\boldsymbol{\psi}_v$, $\boldsymbol{\psi}_{e,q}^t$, $\boldsymbol{\psi}_{e,q}^n$, and $\boldsymbol{\psi}_{K,\boldsymbol{q}}$ are the functions given in (D1)–(D4), respectively. Then, the following hold.

(i) $\boldsymbol{Z}_1, \boldsymbol{Z}_2, \boldsymbol{Z}_3, \boldsymbol{Z}_4 \subset \boldsymbol{Z}_{h,0}$.
(ii) $\boldsymbol{Z}_i \cap \boldsymbol{Z}_j = \{0\}$ *for any pair (i, j) with $i \neq j$.*
(iii) *The dimensions of the subspaces $\boldsymbol{Z}_1$, $\boldsymbol{Z}_2$, $\boldsymbol{Z}_3$, and $\boldsymbol{Z}_4$ satisfy*

$$\dim \boldsymbol{Z}_1 = N_{V,i}, \quad \dim \boldsymbol{Z}_2 = k N_{E,i},$$
$$\dim \boldsymbol{Z}_3 = (k-1) N_{E,i}, \quad \dim \boldsymbol{Z}_4 = \frac{(k-1)(k-2)}{2} N_P.$$

Consequently, $\boldsymbol{Z}_{h,0} = \boldsymbol{Z}_1 \oplus \boldsymbol{Z}_2 \oplus \boldsymbol{Z}_3 \oplus \boldsymbol{Z}_4$.

Proof Since $\boldsymbol{Z}_{h,0} = \boldsymbol{Z}_h \cap \boldsymbol{V}_{h,0}$, and from Lemma 1, it suffices to show that the functions in (D1)–(D4) are contained in $\boldsymbol{V}_{h,0}$. Clearly $\boldsymbol{\psi}_{K,\boldsymbol{q}} \in \boldsymbol{V}_{h,0}$ for any $K \in \mathcal{P}_h$ and any $\boldsymbol{q} \in \boldsymbol{M}_k^{\oplus}$. If $e \in \mathcal{E}_h^i$, then $\boldsymbol{\psi}_{e,q}^t \in \boldsymbol{V}_{h,0}$ for any $q \in M_{k-1}(e)$ and $\boldsymbol{\psi}_{e,q}^n \in \boldsymbol{V}_{h,0}$ for any $q \in M_{k-1}(e) \setminus \{1\}$. If $v \in \mathcal{V}_h^i$, then the edges in $\mathcal{E}_h$ that have v as an end point are contained in $\mathcal{E}_h^i$. Thus, $\boldsymbol{\psi}_v \in \boldsymbol{V}_{h,0}$ for any $v \in \mathcal{V}_h^i$. Hence, $\boldsymbol{Z}_1$, $\boldsymbol{Z}_2$, $\boldsymbol{Z}_3$, and $\boldsymbol{Z}_4$ are subspaces of $\boldsymbol{Z}_{h,0}$.

On the other hand, it is easy to show that $\boldsymbol{Z}_i \cap \boldsymbol{Z}_j = \{0\}$ for any pair (i, j) with $i \neq j$ and

$$\dim \boldsymbol{Z}_1 = N_{V,i}, \quad \dim \boldsymbol{Z}_2 = kN_{E,i},$$
$$\dim \boldsymbol{Z}_3 = (k-1)N_{E,i}, \quad \dim \boldsymbol{Z}_4 = \frac{(k-1)(k-2)}{2} N_P.$$

Then, since $\boldsymbol{Z}_1 \oplus \boldsymbol{Z}_2 \oplus \boldsymbol{Z}_3 \oplus \boldsymbol{Z}_4 \subset \boldsymbol{Z}_{h,0}$ and since $\dim \boldsymbol{Z}_{h,0} = \dim \boldsymbol{Z}_1 + \dim \boldsymbol{Z}_2 + \dim \boldsymbol{Z}_3 + \dim \boldsymbol{Z}_4$ by Proposition 2, we obtain

$$\boldsymbol{Z}_{h,0} = \boldsymbol{Z}_1 \oplus \boldsymbol{Z}_2 \oplus \boldsymbol{Z}_3 \oplus \boldsymbol{Z}_4.$$

This concludes the proof of the theorem. □

Remark 2 If $k = 1$ and the mesh $\mathcal{P}_h$ is a triangular mesh, then the construction of the basis of $\boldsymbol{Z}_{h,0}$ described in Theorem 2 is exactly the same with the divergence-free basis in the Crouzeix-Raviart finite element space [14, 26].

5 Implementation details

In this section, we present how to compute the solution $(\boldsymbol{u}_h, p_h)$ of the discrete problem (8) by using the construction of $\boldsymbol{Z}_{h,0}$ presented in Section 4.

5.1 Computing the discrete velocity u_h

We first consider the case $\boldsymbol{g} = \boldsymbol{0}$. Note that the discrete velocity $\boldsymbol{u}_h$ is the solution of the following discrete problem [18]: Find $\boldsymbol{u}_h \in \boldsymbol{Z}_{h,0}$ such that

$$a_h(\boldsymbol{u}_h, \boldsymbol{v}_h) = \langle \boldsymbol{f}_h, \boldsymbol{v}_h \rangle \quad \forall \boldsymbol{v}_h \in \boldsymbol{Z}_{h,0}. \tag{10}$$

Since $\dim \boldsymbol{Z}_{h,0} = \dim \boldsymbol{V}_{h,0} - \dim Q_h$, the system (10) has a smaller number of unknowns than system (8). Moreover, system (10) is symmetric positive definite, while problem (8) is a saddle point problem. Thus, it is more efficient to compute $\boldsymbol{u}_h$ from (10) than from the problem (8).

We next consider the case $\boldsymbol{g} \neq \boldsymbol{0}$. Let us decompose $\boldsymbol{u}_h \in \boldsymbol{V}_{h,\boldsymbol{g}}$ into

$$\boldsymbol{u}_h = \boldsymbol{u}_{h,0} + \widetilde{\boldsymbol{u}}_h,$$

where $\widetilde{\boldsymbol{u}}_h \in \boldsymbol{V}_{h,\boldsymbol{g}} \cap \boldsymbol{Z}_h$ and $\boldsymbol{u}_{h,0} \in \boldsymbol{Z}_{h,0}$ is the solution of the problem

$$a_h(\boldsymbol{u}_{h,0}, \boldsymbol{v}_h) = \langle \boldsymbol{f}_h, \boldsymbol{v}_h \rangle - a_h(\widetilde{\boldsymbol{u}}_h, \boldsymbol{v}_h) \quad \forall \boldsymbol{v}_h \in \boldsymbol{Z}_{h,0}.$$

Using the construction of $\boldsymbol{Z}_{h,0}$ presented in Theorem 2, we can compute $\boldsymbol{u}_{h,0}$ by solving a symmetric positive definite system of linear equations, as explained in the case $\boldsymbol{g} = \boldsymbol{0}$. It remains to find a function $\widetilde{\boldsymbol{u}}_h \in \boldsymbol{V}_{h,\boldsymbol{g}} \cap \boldsymbol{Z}_h$. The following theorem shows that we can easily find such a function.

Theorem 3 *Let $N = N_V^\partial$ and label the vertices in $\mathcal{V}_h^\partial$ by $1, 2, \cdots, N$ such that $v_1, \cdots, v_N$ are in counterclockwise order with respect to Ω. We also label the edges in $\mathcal{E}_h^\partial$ by $1, 2, \cdots, N$, such that the endpoints of the edge e_i are v_i and v_{i+1} for $i = 1, 2, \cdots, N-1$, and the endpoints of the edge e_N are v_N and v_1 (since Ω is a simply connected polygon, $N_V^\partial = N_E^\partial$). Let $\widetilde{\boldsymbol{u}}_h$ be the function in $\boldsymbol{V}_h$ defined by*

$$\widetilde{\boldsymbol{u}}_h = \sum_{v \in \mathcal{V}_h^\partial} C_{1,v} \boldsymbol{\psi}_v + \sum_{e \in \mathcal{E}_h^\partial} \sum_{q \in M_{k-1}(e)} C_{2,e,q} \boldsymbol{\psi}_{e,q}^t + \sum_{e \in \mathcal{E}_h^\partial} \sum_{q \in M_{k-1}(e) \setminus \{1\}} C_{3,e,q} \boldsymbol{\psi}_{e,q}^n,$$

where the coefficients $(C_{1,v})_v = (C_{1,v_1}, \cdots, C_{1,v_N})$ are given by

$$C_{1,v_k} = -\sum_{i=k}^{N} \int_{e_i} \boldsymbol{g} \cdot \boldsymbol{n}_{e_i} \mathrm{d}s, \quad k = 1, 2, \cdots, N,$$

and the coefficients $(C_{2,e,q})_{e,q}$, and $(C_{3,e,q})_{e,q}$ are given by

$$\begin{aligned} C_{2,e,q} &= \frac{1}{|e|} \int_e \boldsymbol{g} \cdot \boldsymbol{t}_e q \mathrm{d}s, \quad q \in M_{k-1}(e),\ e \in \mathcal{E}_h^\partial, \\ C_{3,e,q} &= \frac{1}{|e|} \int_e \boldsymbol{g} \cdot \boldsymbol{n}_e q \mathrm{d}s, \quad q \in M_{k-1}(e) \setminus \{1\},\ e \in \mathcal{E}_h^\partial. \end{aligned}$$

Then, $\widetilde{\boldsymbol{u}}_h \in \boldsymbol{V}_{h,\boldsymbol{g}} \cap \boldsymbol{Z}_h$.

Proof From the construction of $\widetilde{\boldsymbol{u}}_h$, it is obvious that $\mathrm{div}_h \widetilde{\boldsymbol{u}}_h = 0$. Thus, it remains to show that $\widetilde{\boldsymbol{u}}_h \in \boldsymbol{V}_{h,\boldsymbol{g}}$. From the definition of the coefficients $(C_{2,e,q})_{e,q}$, and $(C_{3,e,q})_{e,q}$, we obtain

$$\begin{aligned} \int_e \widetilde{\boldsymbol{u}}_h \cdot \boldsymbol{t}_e q \mathrm{d}s &= \int_e \boldsymbol{g} \cdot \boldsymbol{t}_e q \mathrm{d}s, \quad q \in M_{k-1}(e),\ e \in \mathcal{E}_h^\partial, \\ \int_e \widetilde{\boldsymbol{u}}_h \cdot \boldsymbol{n}_e q \mathrm{d}s &= \int_e \boldsymbol{g} \cdot \boldsymbol{n}_e q \mathrm{d}s, \quad q \in M_{k-1}(e) \setminus \{1\},\ e \in \mathcal{E}_h^\partial. \end{aligned}$$

Since the boundary edge e_i with $1 \le i \le N-1$ has endpoints v_i and v_{i+1}, and since the vertices $v_1, \cdots, v_N$ are labeled in counterclockwise order with respect to Ω, we obtain

$$\boldsymbol{n}_{e_i, v_{i+1}} = \boldsymbol{n}_{e_i} = -\boldsymbol{n}_{e_i, v_i},$$

where $\boldsymbol{n}_{e_i}$ is a unit normal vector in the outward direction with respect to Ω, and $\boldsymbol{n}_{e_i, v_i}$ and $\boldsymbol{n}_{e_i, v_{i+1}}$ are unit vectors normal to e_i pointing in the counterclockwise direction with respect to v_i and v_{i+1}, respectively (see Fig. 2). Similarly, we obtain

$$\boldsymbol{n}_{e_N, v_1} = \boldsymbol{n}_{e_N} = -\boldsymbol{n}_{e_N, v_N}.$$

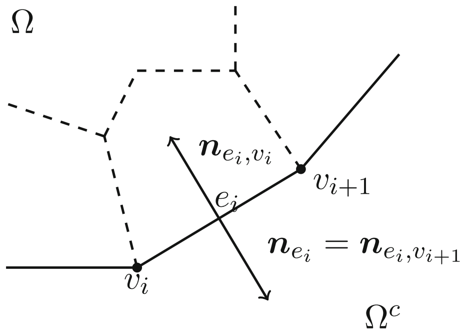

Fig. 2 The normal vectors on the edge e_i

Thus, we have

$$\int_{e_i} \widetilde{\boldsymbol{u}}_h \cdot \boldsymbol{n}_{e_i} \mathrm{d}s = -C_{1,v_i} + C_{1,v_{i+1}} \quad \forall i = 1, 2, \cdots, N-1,$$

$$\int_{e_N} \widetilde{\boldsymbol{u}}_h \cdot \boldsymbol{n}_{e_N} \mathrm{d}s = -C_{1,v_N} + C_{1,v_1}.$$

Using the definition of the coefficients $(C_{1,v})$,

$$-C_{1,v_i} + C_{1,v_{i+1}} = \int_{e_i} \boldsymbol{g} \cdot \boldsymbol{n}_{e_i} \mathrm{d}s \quad \forall i = 1, 2, \cdots, N-1.$$

From (2) we obtain $C_{1,v_1} = -\int_{\partial\Omega} \boldsymbol{g} \cdot \boldsymbol{n}_\Omega \mathrm{d}s = 0$ and thus

$$-C_{1,v_N} + C_{1,v_1} = \int_{e_N} \boldsymbol{g} \cdot \boldsymbol{n}_{e_N} \mathrm{d}s.$$

Therefore $\widetilde{\boldsymbol{u}}_h \in \boldsymbol{V}_{h,\boldsymbol{g}}$. □

5.2 Recovery of the discrete pressure p_h

Once we have the discrete velocity $\boldsymbol{u}_h$, the discrete pressure p_h can be obtained by solving the system

$$b_h(\boldsymbol{v}_h, p_h) = \langle \boldsymbol{f}_h, \boldsymbol{v}_h \rangle - a_h(\boldsymbol{u}_h, \boldsymbol{v}_h) \quad \forall \boldsymbol{v}_h \in \boldsymbol{V}_{h,0}. \tag{11}$$

This can be rewritten as an overdetermined linear system

$$\underline{\mathbf{B}}\underline{\mathbf{p}} = \underline{\mathbf{f}} \tag{12}$$

where $\underline{\mathbf{B}}$ is a $\dim(\boldsymbol{V}_{h,0}) \times \dim(Q_h)$ matrix. Since $b_h(\cdot,\cdot)$ satisfies the inf-sup condition and since the discrete problem (8) is well-posed, the matrix $\underline{\mathbf{B}}$ has full rank and the linear system (12) has the unique solution. Note that this solution also solves the normal equation

$$\underline{\mathbf{B}}^\intercal \underline{\mathbf{B}}\underline{\mathbf{p}} = \underline{\mathbf{B}}^\intercal \underline{\mathbf{f}}. \tag{13}$$

Since the matrix $\underline{\mathbf{B}}$ has full rank, the normal (13) is a symmetric positive definite linear system. Thus, (13) has only one solution, which is also the solution of (12).

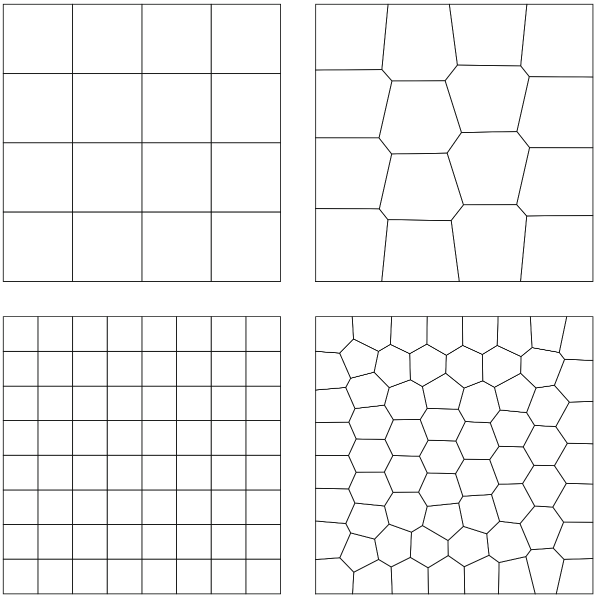

Fig. 3 The meshes $\mathcal{P}_h^1$ (left), and $\mathcal{P}_h^2$ (right)

6 Numerical experiments

In this section, we present several numerical experiments for the symmetric positive definite linear system (10) and the overdetermined linear system (11). Consider the Stokes problem (1) on the unit square domain $\Omega = [0, 1]^2$, where the exact solution is given by

$$\begin{aligned} \boldsymbol{u}(x, y) &= ((1 - \cos(2\pi x)) \sin(2\pi y), -(1 - \cos(2\pi y)) \sin(2\pi x)), \\ p(x, y) &= xy^2 - \frac{1}{6}. \end{aligned}$$

Table 1 Mesh information

h	$\mathcal{P}_h^1$			$\mathcal{P}_h^2$		
	N_P	$N_{E,i}$	$N_{V,i}$	N_P	$N_{E,i}$	$N_{V,i}$
1/4	16	24	9	16	33	18
1/8	64	112	49	64	162	99
1/16	256	480	225	256	707	452
1/32	1024	1984	961	1024	2953	1930
1/64	4096	8064	3969	4096	12043	7948
1/128	16384	32512	16129	16384	48655	32272

Table 2 Dimensions of the discrete spaces ($k = 1$)

h	$\mathcal{P}_h^1$			$\mathcal{P}_h^2$		
	dim $\boldsymbol{V}_{h,0}$	dim Q_h	dim $\boldsymbol{Z}_{h,0}$	dim $\boldsymbol{V}_{h,0}$	dim Q_h	dim $\boldsymbol{Z}_{h,0}$
1/4	48	15	33	66	15	51
1/8	224	63	161	324	63	261
1/16	960	255	705	1414	255	1159
1/32	3968	1023	2945	5906	1023	4883
1/64	16128	4095	12033	24086	4095	19991
1/128	65024	16383	48641	97310	16383	80927

We solve both (10) and (11) for $k = 1, 2, 3$, and we compute the velocity error in the discrete energy norm

$$E_v := a_h(\boldsymbol{u}_h - I_h\boldsymbol{u}, \boldsymbol{u}_h - I_h\boldsymbol{u})^{1/2}$$

and the pressure error in the L^2-norm

$$E_p := \|p_h - \Pi_h p\|_{0,\Omega},$$

where $\Pi_h p$ is the piecewise polynomial function such that for each $K \in \mathcal{P}_h$ the restriction $\Pi_h p|_K$ is the L^2-projection of p onto $P_{k-1}(K)$.

We decompose Ω into the following sequences of convex polygonal meshes:

(i) uniform square meshes $\mathcal{P}_h^1$ with $h = 1/4, 1/8, 1/16, 1/32, 1/64, 1/128$,
(ii) unstructured polygonal meshes $\mathcal{P}_h^2$ with $h = 1/4, 1/8, 1/16, 1/32, 1/64, 1/128$.

Some examples of the meshes are shown in Fig. 3. The unstructured polygonal meshes $\{\mathcal{P}_h^2\}_h$ are generated from PolyMesher [24]. Mesh data (the number of polygons, interior edges, and interior vertices) for each h are given in Table 1.

In Tables 2, 3 and 4, we present the dimensions of the spaces $\boldsymbol{V}_{h,0}$, Q_h, and $\boldsymbol{Z}_{h,0}$, for each mesh $\mathcal{P}_h^1$, $\mathcal{P}_h^2$ and each $k = 1, 2, 3$. Since the number of unknowns of the

Table 3 Dimensions of the discrete spaces ($k = 2$)

h	$\mathcal{P}_h^1$			$\mathcal{P}_h^2$		
	dim $\boldsymbol{V}_{h,0}$	dim Q_h	dim $\boldsymbol{Z}_{h,0}$	dim $\boldsymbol{V}_{h,0}$	dim Q_h	dim $\boldsymbol{Z}_{h,0}$
1/4	128	47	81	164	47	117
1/8	576	191	385	776	191	585
1/16	2432	767	1665	3340	767	2573
1/32	9984	3071	6913	13860	3071	10789
1/64	40448	12287	28161	56364	12287	44077
1/128	162816	49151	113665	227388	49151	178237

Table 4 Dimensions of the discrete spaces ($k = 3$)

h	$\mathcal{P}_h^1$			$\mathcal{P}_h^2$		
	dim $\boldsymbol{V}_{h,0}$	dim Q_h	dim $\mathbf{Z}_{h,0}$	dim $\boldsymbol{V}_{h,0}$	dim Q_h	dim $\mathbf{Z}_{h,0}$
1/4	240	95	145	294	95	199
1/8	1056	383	673	1356	383	973
1/16	4416	1535	2881	5778	1535	4243
1/32	18048	6143	11905	23862	6143	17719
1/64	72960	24575	48385	96834	24575	72259
1/128	293376	98303	195073	390234	98303	291931

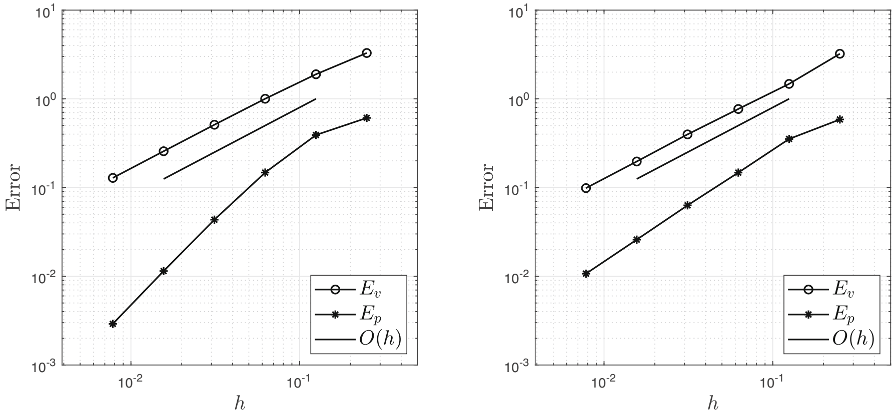

Fig. 4 Error curves with respect to h for the velocity and pressure on the sequences of meshes $\mathcal{P}_h^1$ (left) and $\mathcal{P}_h^2$ (right) with $k = 1$

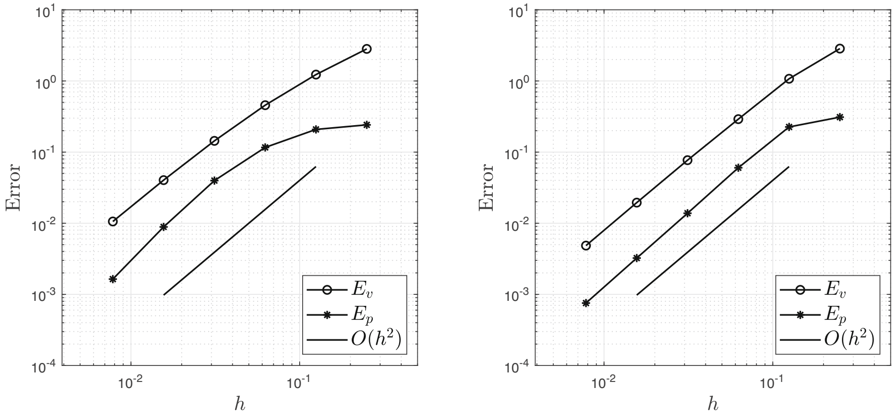

Fig. 5 Error curves with respect to h for the velocity and pressure on the sequences of meshes $\mathcal{P}_h^1$ (left) and $\mathcal{P}_h^2$ (right) with $k = 2$

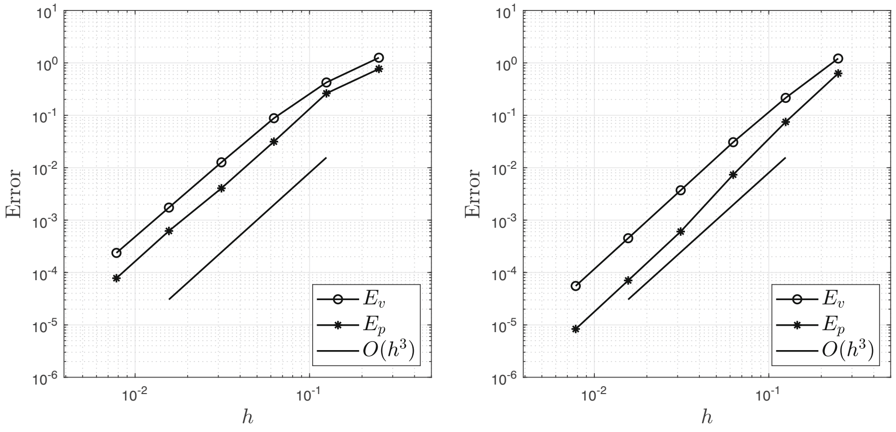

Fig. 6 Error curves with respect to h for the velocity and pressure on the sequences of meshes $\mathcal{P}_h^1$ (left) and $\mathcal{P}_h^2$ (right) with $k = 3$

system (8) is $\dim \boldsymbol{V}_{h,0} + \dim Q_h$ and the number of unknowns of the system (10) is $\dim \boldsymbol{Z}_{h,0}$, we can see that the system (10) has fewer unknowns than the system (8).

The errors E_v and E_p and their orders on the sequences of the meshes for $k = 1, 2, 3$ are given in Figs. 4, 5 and 6. In these figures, we see that the convergence order of the errors E_v and E_p are $O(h^k)$ for $k = 1, 2, 3$. Thus, the numerical results confirm the theoretical analysis in Theorem 1.

In Table 5, we compare the CPU running times (on a PC with an Intel Core i5 processor and 16GB RAM) required to solve the reduced system (10) and the original saddle point system (8), for the uniform square meshes $\{\mathcal{P}_h^1\}_h$ and $k = 1, 2, 3$. For a fair comparison, we use unpreconditioned conjugate gradient method (CG) to solve (10) and the standard Uzawa method to solve (8). The cost for computing the discrete pressure (by solving (11)) is a fraction of CG; hence, it is not included. For each

Table 5 CPU running times

h	CPU time (secs)					
	$k = 1$		$k = 2$		$k = 3$	
	CG	Uzawa	CG	Uzawa	CG	Uzawa
1/4	0.0002	0.030	0.001	0.829	0.004	18.636
1/8	0.0009	0.692	0.006	12.761	0.034	349/386
1/16	0.0090	11.567	0.029	304.348	0.389	5732.469
1/32	0.0810	338.71	0.392	7644.293	4.255	$*$
1/64	1.5880	10152.847	7.191	$*$	53.712	$*$
1/128	26.999	$*$	93.194	$*$	721.477	$*$

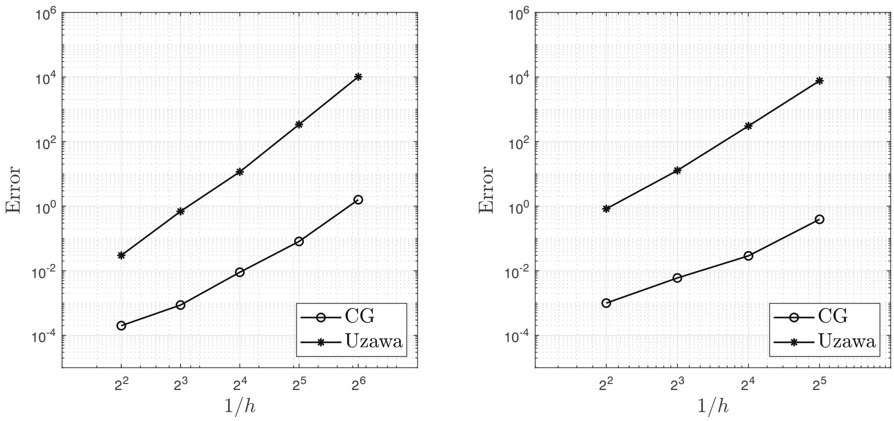

Fig. 7 CPU time curves of CG and Uzawa with respect to $1/h$ with $k = 1$ (left) and $k = 2$ (right)

experiment, we write “$*$” if the CPU time is more than 12,000 s. For all cases, the CPU time of solving the reduced system is much smaller than that of solving the saddle point system (Fig. 7).

7 Conclusions

We presented a formal construction of divergence-free bases in the nonconforming VEM for solving the stationary Stokes problem on arbitrary polygonal meshes introduced in [29]. If $k = 1$ and the mesh is triangular, then the proposed construction of the basis is exactly the same as the divergence-free basis in the Crouzeix-Raviart finite element space [14, 26]. Using our construction, we are able to eliminate the pressure variable from the discrete saddle point formulation, and reduce it to a symmetric positive definite linear system in the velocity variable only. Thus, we can apply many efficient solvers available for symmetric positive definite systems. Finally, we provided some numerical experiments confirming the theoretical results and the efficiency of our construction of divergence-free bases in the nonconforming VEM for the Stokes problem.

Funding This work is partially supported by NRF, contract no. 2021R1A2C1003340.

Availability of data and materials Data sharing not applicable to this article as no datasets were generated or analyzed during the current study.

Declarations

Conflict of interest The authors declare no competing interests.

References

1. Ahmad, B., Alsaedi, A., Brezzi, F., Marini, L.D., Russo, A.: Equivalent projectors for virtual element methods. Comput. Math. Appl. **66**(3), 376–391 (2013)
2. Antonietti, P.F., Beirão da Veiga, L., Mora, D., Verani, M.: A stream virtual element formulation of the Stokes problem on polygonal meshes. SIAM J. Numer. Anal. **52**(1), 386–404 (2014)
3. Antonietti, P.F., Manzini, G., Verani, M.: The fully nonconforming virtual element method for biharmonic problems. Math. Models Methods Appl. Sci. **28**(2), 387–407 (2018)
4. de Dios, B.A., Lipnikov, K., Manzini, G.: The nonconforming virtual element method. ESAIM Math. Model. Numer. Anal. **50**(3), 879–904 (2016)
5. Beirão da Veiga, L., Brezzi, F., Cangiani, A., Manzini, G., Marini, L.D., Russo, A.: Basic principles of virtual element methods. Math. Models Methods Appl. Sci. **23**(1), 199–214 (2013)
6. Beirão da Veiga, L., Brezzi, F., Dassi, F., Marini, L.D., Russo, A.: Virtual element approximation of 2D magnetostatic problems. Comput. Methods Appl. Mech Engrg. **327**, 173–195 (2017)
7. Beirão da Veiga, L., Brezzi, F., Dassi, F., Marini, L.D., Russo, A.: A family of three-dimensional virtual elements with applications to magnetostatics. SIAM J. Numer. Anal. **56**(5), 2940–2962 (2018)
8. Beirão da Veiga, L., Brezzi, F., Dassi, F., Marini, L.D., Russo, A.: Lowest order virtual element approximation of magnetostatic problems. Comput. Methods Appl. Mech. Engrg. **332**, 343–362 (2018)
9. Beirão da Veiga, L., Brezzi, F., Marini, L.D.: Virtual elements for linear elasticity problems. SIAM J. Numer. Anal. **51**(2), 794–812 (2013)
10. Beirão da Veiga, L., Brezzi, F., Marini, L.D., Russo, A.: The hitchhiker's guide to the virtual element method. Math. Models Methods Appl. Sci. **24**(8), 1541–1573 (2014)
11. da Veiga, L.B., Brezzi, F., Marini, L.D., Russo, A.: Mixed virtual element methods for general second order elliptic problems on polygonal meshes. ESAIM Math. Model. Numer. Anal. **50**(3), 727–747 (2016)
12. da Veiga, L.B., Lovadina, C., Vacca, G.: Divergence free virtual elements for the Stokes problem on polygonal meshes. ESAIM Math. Model. Numer. Anal. **51**(2), 509–535 (2017)
13. da Veiga, L.B., Dassi, F., Manzini, G., Mascotto, L.: Virtual elements for Maxwell's equations. Comput. Math. Appl. In press (2021)
14. Brenner, S.C.: A nonconforming multigrid method for the stationary Stokes equations. Math. Comp. **55**(192), 411–437 (1990)
15. Brezzi, F., Falk, R.S.: Basic principles of mixed virtual element methods. ESAIM Math. Model. Numer. Anal. **48**(4), 1227–1240 (2014)
16. Cangiani, A., Gyrya, V., Manzini, G.: The nonconforming virtual element method for the Stokes equations. SIAM J. Numer. Anal. **54**(6), 3411–3435 (2016)
17. Cangiani, A., Manzini, G., Sutton, O.J.: Conforming and nonconforming virtual element methods for elliptic problems. IMA J. Numer. Anal. **37**(3), 1317–1354 (2017)
18. Crouzeix, M., Raviart, P.-A.: Conforming and nonconforming finite element methods for solving the stationary Stokes equations. I. Rev. Française Automat. Informat. Recherche Opérationnelle Sér. Rouge **7**(R-3), 33–75 (1973)
19. Beirão da Veiga, L., Brezzi, F., Marini, L.D., Russo, A.: $H(\mathrm{div})$ and $h(\mathbf{curl})$-conforming virtual element methods. Numer. Math. **133**(2), 303–332 (2016)
20. Gardini, F., Manzini, G., Vacca, G.: The nonconforming virtual element method for eigenvalue problems. ESAIM Math. Model. Numer. Anal. **53**(3), 749–774 (2019)
21. Gardini, F., Vacca, G.: Virtual element method for second-order elliptic eigenvalue problems. IMA J. Numer. Anal. **38**(4), 2026–2054 (2018)
22. Do, Y., Park, H.: Lowest-order virtual element methods for linear elasticity problems. Comput. Methods Appl. Mech. Kwak Eng. **390**:Paper No 114448 (2022)
23. Liu, X., Li, J., Chen, Z.: A nonconforming virtual element method for the Stokes problem on general meshes. Comput. Methods Appl. Mech. Eng. **320**, 694–711 (2017)
24. Talischi, C., Paulino, G.H., Pereira, A., Menezes, I.F.M.: `PolyMesher`: a general-purpose mesh generator for polygonal elements written in Matlab. Struct. Multidiscip. Optim. **45**(3), 309–328 (2012)
25. Tang, X., Liu, Z., Zhang, B., Feng, M.: A low-order locking-free virtual element for linear elasticity problems. Comput. Math. Appl. **80**(5), 1260–1274 (2020)
26. Thomasset, F.: Implementation of finite element methods for Navier-Stokes equations. Springer Series in Computational Physics. Springer, New York-Berlin (1981)

27. Zhang, B., Zhao, J., Yang, Y., Chen, S.: The nonconforming virtual element method for elasticity problems. J. Comput. Phys. **378**, 394–410 (2019)
28. Zhao, J., Zhang, B., Chen, S., Mao, S.: The Morley-type virtual element for plate bending problems. J. Sci. Comput. **76**(1), 610–629 (2018)
29. Zhao, J., Zhang, B., Mao, S., Chen, S.: The divergence-free nonconforming virtual element for the Stokes problem. SIAM J. Numer. Anal. **57**(6), 2730–2759 (2019)